Exploring Chemical Composition Changes in *Pinellia* Tuber via Ginger–Aluminum Potassium Sulfate Processing

Yuting YANG,* Yuto NISHIDONO,† Tohru KAMITANAKA,‡ Ken TANAKA§

Abstract: Despite its recognized expectorant, antitussive, and antiemetic effects, *Pinellia* tuber (PT) requires processing to mitigate its toxicity and irritation prior to clinical application. Traditional PT processing methods include hot water washing and ginger–aluminum potassium sulfate (G-APS) treatment, each historically applied for distinct therapeutic purposes. Additional processing approaches have emerged in recent years, with reported compositional changes. However, the clinical relevance of traditional methods remains unclear. Among the chemical constituents of PT, lysophosphatidylcholines (LPCs) have garnered significant attention for their gastroprotective effects and pro-inflammatory activity. Although LPCs are pharmacologically significant, the influence of processing on their levels and the resulting effects of changes in their levels on the clinical utility of PT remain poorly understood. This study characterized chemical changes in PT induced by traditional processing and investigated the implications for detoxification and therapeutic applications. In this study, PT samples were subjected to no processing (control), hot water washing, or G-APS boiling, followed by chemical composition analysis using liquid chromatography–quadrupole time-of-flight tandem mass spectrometry. The metabolic profile of hot-water-treated PT samples resembled that of untreated samples, with hot water treatment primarily exerting a quantitative effect on LPC content. Conversely, G-APS processing induced both quantitative and qualitative changes in LPC content. The study findings illustrate that different processing methods generate distinct chemical profiles in PT, particularly concerning phospholipid content, highlighting the need to align processing selection with detoxification goals and therapeutic intent for efficacy and safety assurance. Thus, the treatment of crude drugs for detoxification purposes requires careful planning, as this process could simultaneously lead to a reduction in therapeutic efficacy.

Keywords: *Pinellia tuber, ginger, aluminum potassium sulfate processing, lysophosphatidylcholine, lysophosphatidylethanolamine, LC–MS*

1. Introduction

* Doctoral Student, College of Pharmaceutical Sciences, Ritsumeikan University

† Assistant Professor, College of Pharmaceutical Sciences, Ritsumeikan University

‡ Assistant Professor, College of Pharmaceutical Sciences, Ritsumeikan University

§ Professor, College of Pharmaceutical Sciences, Ritsumeikan University

Email: * gr0635rx@ed.ritsumei.ac.jp

† nisidono@fc.ritsumei.ac.jp

‡ t-kmtnk@fc.ritsumei.ac.jp

§ ktanaka@fc.ritsumei.ac.jp

Received on June 16, accepted after peer reviews on November 20; published online: December 25, 2025

Asia-Japan Research Academic Bulletin, 2025

ONLINE ISSN 2435-306X, Vol.6, 35

Pinellia tuber (PT), the dried tuber of *Pinellia ternata* Breitenbach (Araceae), is listed as a crude drug in the Japanese Pharmacopoeia 18th Edition (Ministry of Health, Labour and Welfare 2021) and Chinese Pharmacopoeia 2020 Edition (Chinese Pharmacopoeia Commission 2020). PT is widely prescribed in the classical formulas of Traditional Japanese Kampo and Chinese Medicine for expectorant, antitussive, and antiemetic purposes (Bai et al. 2022; Suzuki et al. 2009). However, it exhibits inherent toxicity and mucosal irritancy, with reported adverse effects, including inflammation, teratogenicity, cardiotoxicity, and conjunctival irritation (Peng et al. 2022; Su et al. 2016a; Zhang et al. 2013). Therefore, proper PT processing is required before clinical application to ensure safety.

Among traditional processing methods, hot water washing (湯洗) has been used for centuries to reduce PT-induced toxicity. This method was recorded in volumes such as *Jin Gui Yu Han Jing* (Classic of the Golden Chamber and Jade Case, 金匱玉函經) and *Ben Cao Jing Ji Zhu* (Collective Commentaries on Classics of Materia Medica, 本草經集注) (Chinese Text Project n.d.a; Chinese Text Project n.d.b). Moreover, the use of ginger as an adjuvant based on hot water washing is summarized in *Liu Juan Zi Gui Yi Fang* (Liu Juanzi's Ghost-Bequeathed Prescriptions, 劉涓子鬼遺方) (Chinese Text Project n.d.c). With advances in processing technology, increasingly complex methods have been applied to PT. *Ying Tong Bai Wen* (A Hundred Questions about Infants and Children, 嬰童百問) and *Wan Bing Hui Chun* (Restoration of Health from the Myriad Diseases, 萬病回春) document the method of boiling PT with ginger and aluminum potassium sulfate (G-APS) for detoxification purposes (Chinese Text Project n.d.d; Chinese Text Project n.d.e). In modern PT processing, the Chinese Pharmacopoeia 2020 edition summarizes three official processing methods: *Pinelliae Rhizoma cum Alumine* (processed with aluminum potassium sulfate), *Pinelliae Rhizoma cum Zingibere et Alumine* (processed with G-APS), and *Pinelliae Rhizoma Praeparatum* (processed with *Glycyrrhiza uralensis* and calcium oxide) (Chinese Pharmacopoeia Commission 2020).

G-APS processing has received considerable attention because of its longstanding historical use. G-APS processing reduces the levels of various chemical constituents in PT, such as alkaloids, nucleosides, organic acids, amino acids, lipid components, and saccharides (Lee et al. 2016; Li et al. 2022; Shi et al. 2024; Su et al. 2016b). Makino's group demonstrated that heating or ginger extract treatment denatures calcium oxalate crystals and reduces the associated content of toxic *P. ternata* lectin (Fueki et al. 2022; Fueki et al. 2020; Liu et al. 2023). Although these findings offer valuable insight into G-APS processing, most studies have focused on reducing the content of irritants such as calcium oxalate crystals and lectins. Recently, Afroz *et al.* reported that PT contains large amounts of phospholipids (Afroz et al. 2018). Lysophosphatidylcholines (LPCs), a class of slightly water-soluble, amphiphilic phospholipids, have recently attracted attention for their roles as inflammatory mediators and for their bidirectional pharmacological effects in humans (Ahmad et al. 2015). In plasma, LPCs are metabolized by autotaxin (ATX) to lysophosphatidic acid (LPA), a bioactive lipid mediator that protects against indomethacin-induced gastric epithelial injury, thereby conferring gastroprotective effects (Afroz et al. 2018; Nakanaga et al. 2010). Conversely, LPCs promote inflammatory responses by inducing the production of pro-inflammatory mediators, thereby supporting the progression of inflammatory diseases (Liu et al. 2020; Matsumoto et al. 2007). These bidirectional pharmacological effects are of particular interest, as they can exert opposing influences on the two principal clinical applications of PT, namely, its antiemetic and expectorant functions. However, the effects of processing on the phospholipid content of PT have not been examined, and the link between processing-induced chemical changes and PT's pharmacological efficacy remains unclear.

Given the rising clinical demand for PT, ensuring the quality, safety, and efficacy of processed PT products is critical. Therefore, clarifying processing-induced chemical changes is essential to

optimize therapeutic efficacy and safety. This study investigated the phospholipid content of PT, especially LPCs, after hot water washing and G-APS processing. Key compounds affected by processing were annotated, and their relationships with detoxification and therapeutic efficacy were investigated through a comparison analysis of chemical profiles pre- and post-processing using liquid chromatography–tandem mass spectrometry (LC–MS/MS).

2. Experimental

(1) Materials

Aluminum potassium sulfate 12-water was purchased from Nacalai Tesque, Inc. (Kyoto, Japan). Formic acid (LC–MS-grade) was purchased from FUJIFILM Wako Pure Chemical Corporation (Osaka, Japan). Other analytical-grade chemicals and chromatographic solvents (LC–MS-grade) were purchased from either FUJIFILM Wako Pure Chemical Corporation or Nacalai Tesque, Inc.

(2) Plant Materials

The crude drug specimens of PT were obtained from Tochimoto Tenkaido Co., Ltd. (Osaka, Japan). Yamamotoya (Shiga, Japan) supplied fresh ginger rhizomes. The voucher specimens were stored in the Laboratory of Pharmacognosy, College of Pharmaceutical Sciences, Ritsumeikan University (Shiga, Japan).

(3) Crude Drug Processing

Dried PTs were divided into three groups: a control group without processing and two groups processed by different methods. The processing methods were adapted from previous studies with minor modifications (Chinese Pharmacopoeia Commission 2020; Li et al. 2021; Su et al. 2016b). Each group was prepared in quintuplicate.

For hot water washing, dried PTs (30 g) were soaked in 120 mL of water at 80 °C. Once the temperature dropped to 45°C, the PTs were agitated for 35 min. This washing cycle was repeated 10 times, ensuring that the water remained clear. The PTs were then removed and sun-dried to obtain hot water washing samples (Li et al. 2021).

For G-APS processing, dried PTs (30 g) were soaked in 120 mL of water for 9.5 h until no dry core remained. Fresh ginger was cut into small pieces and squeezed twice with an appropriate volume of distilled water to prepare ginger juice. The resulting juice was adjusted to a ratio of 1 mL/g of fresh ginger. Then, 7.5 mL of fresh ginger juice and 3.75 g of aluminum potassium sulfate were added to 120 mL of water. The PTs were boiled in this mixture for 6 h. After boiling, the samples were removed and sun-dried to obtain the processing samples (Chinese Pharmacopoeia Commission 2020; Su et al. 2016b).

(4) Extract and Sample Solution Preparation

All samples from the three groups were pulverized using a Vita-Mix® ABSOLUTE blender (Model VM0113, Vita-Mix Corp., Cleveland, OH, USA) before extraction. Sample powders (10 g) were extracted with 15 mL of methanol under reflux conditions for 1 h, followed by cooling and filtration. The residues were supplemented with 15 mL of methanol and processed similarly. After

extraction, the filtrates of each sample were combined, and methanol was removed to obtain the extracts. The extracts were accurately weighed and dissolved in methanol to prepare the sample solutions at a concentration of 10 mg/mL. All sample solutions were filtered through a 0.20-μm PTFE membrane and stored at 4°C until further analysis.

(5) Assay of Chemical Constituents Using LC–Quadrupole Time-of-Flight (QTOF)–MS/MS Analysis

LC–QTOF–MS/MS analyses were performed using an Xevo G2–XS QTOF mass spectrometer (Waters, Milford, MA, USA) equipped with an electrospray ionization (ESI) source in both the positive and negative ion modes. The ESI parameters were as follows: data acquisition mode, MS^E; MS^E collision energy, 20–50 eV; acquisition mass range, 50–1,500 Da; cone voltage, 35 eV; capillary voltage, 2.5 kV; source temperature, 150°C; desolvation temperature, 400°C; cone gas flow, 50.0 L/h; and desolvation gas flow, 800 L/h.

A TOSOH TSKgel ODS-100V column (2.0 × 150 mm, 3 μm; Tosoh Bioscience, Tokyo, Japan) was used at a temperature of 40°C. The mobile phase was a binary eluent of (A) water containing 0.1% formic acid and (B) acetonitrile containing 0.1% formic acid under the following gradient conditions: 0–5 min, linear gradient from 20% to 45% B; 5–25 min, linear gradient from 45% to 65% B; 25–40 min, linear gradient from 65% to 85% B; 40–60 min, linear gradient from 85% to 100% B; 60–62 min, isocratic at 100% B; 62–62.1 min, linear gradient from 100% to 20% B; and 62.1–70 min, isocratic at 20% B. The flow rate was 0.3 mL/min.

(6) Data Processing

The raw data generated by LC–QTOF–MS/MS were initially converted into an analysis base file format using Analysis Base File Converter. The analysis base files were then imported into MS-Dial (ver. 5.5; https://systemsomicslab.github.io/compms/msdial/main.html) for comprehensive data processing, including peak extraction, peak deconvolution, peak alignment between samples, ion species annotation, and spectral analysis. In this manner, a list containing information on each detected feature, such as retention time, precursor *m/z*, and MS/MS fragment ions, was generated. The MS-Dial parameters were set as follows: MS1 accurate mass tolerance, 0.01 Da; MS/MS accurate mass tolerance, 0.025 Da; retention time range, 0–100 min; mass range, 0–2,000 Da; minimum peak height, 10,000 amplitudes; mass slice width, 0.1 Da; smoothing level, three scans; minimum peak width, five scans; sigma window value, 0.5; MS/MS abundance cutoff, 500 amplitudes; alignment retention time tolerance, 0.2 min; and alignment MS1 accurate mass tolerance, 0.025 Da.

(7) Statistical Analysis

The peak area values obtained by LC–QTOF–MS/MS in the three groups were analyzed by one-way analysis of variance using Microsoft Excel 2021 (Microsoft, Redmond, WA, USA), with $p < 0.05$ denoting statistical significance.

3. Results and Discussion

(1) Amount of Methanol Extract Obtained from Processed PT

Table 1 presents the amount of methanol extract obtained from PT after processing. The yield was significantly reduced after hot-water washing, whereas G-APS processing did not lead to a noticeable decrease. Hot-water washing, which involves repeated rinsing with large volumes of heated water, is believed to cause substantial leaching of water-soluble components.

Table 1. Extraction Yield in the Three Groups.

Groups	Extraction yield (mg) from 10 g of PT
Control group	231.34 ± 13.01
Hot-water washing group	82.04 ± 5.72
G-APS processing group	266.34 ± 40.29

*Data are presented as the mean ± standard deviation of quintuplicate experiments.

(2) LC–QTOF–MS/MS of PT and Its Processing Products

The chemical constituents of PT and its processed products were analyzed using LC–QTOF–MS/MS. Figure 1 shows the representative total ion chromatograms (TICs) of the three groups in the positive ion mode. With the optimized chromatographic and MS parameters, most PT constituents were successfully detected and separated within 65 min. Analysis of the exact mass number of peaks detected and compositional calculations revealed that phospholipids were eluted at 10–20 min. The LPC profile of the hot water washing group was highly similar to that of the control group, suggesting that this treatment did not induce qualitative changes in LPC composition despite the observed reduction in the yield. Conversely, G-APS–treated PT exhibited marked alterations in the LPC profile, indicating substantial modifications in both the composition and abundance of LPCs.

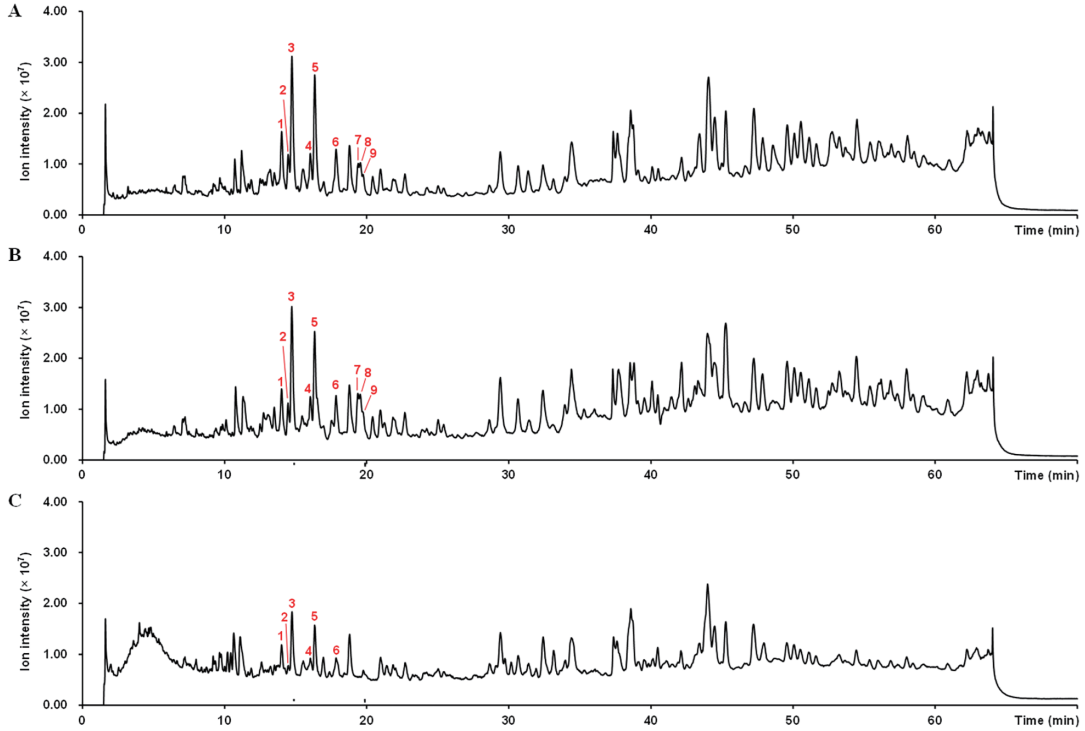

Figure 1. Total Ion Chromatograms of PT and Its Processed Products.

(A) Control group. (B) Hot water washing group. (C) G-APS processing group.

*Note: Peak numbers correspond to those in Table 2.

(3) Annotation of Differential Compounds in PT and Its Processed Products

Based on mass spectral analysis, phospholipids were preliminarily identified using their characteristic fragment ions, and nine peaks exhibiting significant changes in intensity within the elution time for phospholipids were selected for further identification. Most of these compounds were annotated as LPCs and lysophosphatidylethanolamines (LPEs). Table 2 provides detailed information on the compounds and their annotation, including retention times, fragment ions, compound names, molecular formulas, and classifications, among the three groups. Table 3 presents the peak area values obtained by LC–QTOF–MS/MS (n = 5 per group) and the *p*-values among the three groups. Figure 2 presents the corresponding chemical structures.

Table 2. Annotation of Chemical Constituents in PT Before and After Processing.

No.	t_R (min)	Compound	Molecular formula	Mean measured mass (Da)	Theoretical exact mass (Da)	Error (ppm)	Molecular species	Fragment ion mass (*m/z*)
Positive ion mode								
1	14.02	LPC (0:0/18:2)	$C_{26}H_{50}NO_7P$	520.3360	520.3403	7.37	$[M + H]^+$	337.2750 $[M + H - 183]^+$, 184.0750 $[M + H - 336]^+$, 125.0006 $[M + H - 336 - 59]^+$, 86.0971 $[M + H - 336 - 98]^+$
2	14.47	3-{[(2-Aminoethoxy) (hydroxy) phosphoryl] oxy}-2-hydroxypropyl octadecadienoate	$C_{23}H_{44}NO_7P$	478.2962	478.2934	1.22	$[M + H]^+$	460.2817 $[M + H - 18]^+$, 337.2734 $[M + H - 141]^+$
3	14.74	LPC (18:2/0:0)	$C_{26}H_{50}NO_7P$	520.3438	520.3403	3.14	$[M + H]^+$	337.2748 $[M + H - 183]^+$, 184.0743 $[M + H - 336]^+$, 125.0006 $[M + H - 336 - 59]^+$, 104.1077 $[M + H - 416]^+$, 86.0972 $[M + H - 336 - 98]^+$
4	16.04	3-{[(2-Aminoethoxy) (hydroxy)phosphoryl] oxy}-2-hydroxypropyl hexadecanoate	$C_{21}H_{44}NO_7P$	454.2961	454.2934	0.40	$[M + H]^+$	393.2513 $[M + H - 61]^+$, 313.2729 $[M + H - 141]^+$
5	16.35	LPC (16:0/0:0)	$C_{24}H_{50}NO_7P$	496.3418	496.3403	3.49	$[M + H]^+$	478.3308 $[M + H - 18]^+$, 313.2744 $[M + H - 183]^+$, 184.0740 $[M + H - 312]^+$, 125.0006 $[M + H - 312 - 59]^+$, 104.1077 $[M + H - 392]^+$, 86.0971 $[M + H - 312 - 98]^+$
6	17.84	LPC (18:1/0:0)	$C_{26}H_{52}NO_7P$	522.3630	522.3560	2.65	$[M + H]^+$	504.3464 $[M + H - 18]^+$, 339.2887 $[M + H - 183]^+$, 184.0743 $[M + H - 338]^+$, 125.0006 $[M + H - 338 - 59]^+$, 104.1076 [M + H − 418]+, 86.0970 $[M + H - 338 - 98]^+$
Negative ion mode								
7	19.34	Hydroxyoctadecadienoic acid	$C_{18}H_{32}O_3$	295.2300	295.2279	3.83	$[M - H]^-$	295.23294, 277.22198, 255.23708, 225.01091, 195.14212, 183.01501, 171.10567, 119.05238
8	19.53	Hydroxyoctadecadienoic acid	$C_{18}H_{32}O_3$	295.2284	295.2279	4.51	$[M - H]^-$	295.23297, 277.22189, 255.23679, 225.06343, 195.14267, 183.01509, 171.10529 119.0521
9	19.73	Hydroxyoctadecadienoic acid	$C_{18}H_{32}O_3$	295.2276	295.2279	−1.59	$[M - H]^-$	295.23315, 277.22235, 255.23709, 225.06323, 195.14275, 183.01547, 171.10571, 119.05235

Table 3. Peak Area Values of Chemical Constituents in PT Before and After Processing.

No.	t_R (min)	Groups			*p*
		Control group	Hot water washing group	G-APS processing group	
Positive ion mode					
1	14.02	32,086,808.07 ± 2,642,395.34	32,155,610.15 ± 3,958,537.85	3,183,610.64 ± 1,456,998.20	1.62×10^{-9}
2	14.47	32,189,612.24 ± 2,305,627.21	33,314,373.21 ± 3,358,814.74	3,904,996.19 ± 1,703,661.33	4.16×10^{-10}
3	14.74	85,962,086.60 ± 2,458,157.45	88,549,298.10 ± 4,537,646.47	36,759,455.60 ± 13,838,660.59	6.44×10^{-7}
4	16.04	37,5688,81.98 ± 2,043,927.52	38,522,552.83 ± 2,093,793.53	4,394,884.75 ± 1,833,106.48	3.76×10^{-12}
5	16.35	95,268,740.79 ± 5,217,936.65	102,014,569.47 ± 4,049,898.10	26,414,755.80 ± 10,347,375.10	1.36×10^{-9}
6	17.84	64,736,024.54 ± 3,876,925.86	71,843,862.30 ± 7,895,371.65	9,253,076.25 ± 4,126,341.31	9.13×10^{-10}
Negative ion mode					
7	19.34	641,518.59 ± 102,141.86	825,365.31 ± 55,938.85	9,621.66 ± 3,730.50	5.71×10^{-10}
8	19.53	310,482.20 ± 45,212.43	530,902.52 ± 42,273.97	0	8.79×10^{-11}
9	19.73	145,013.43 ± 27,107.02	267,480.46 ± 22,237.95	0	3.62×10^{-10}

*Data are presented as the mean ± standard deviation of quintuplicate experiments. Statistical significance is denoted by $p < 0.05$.

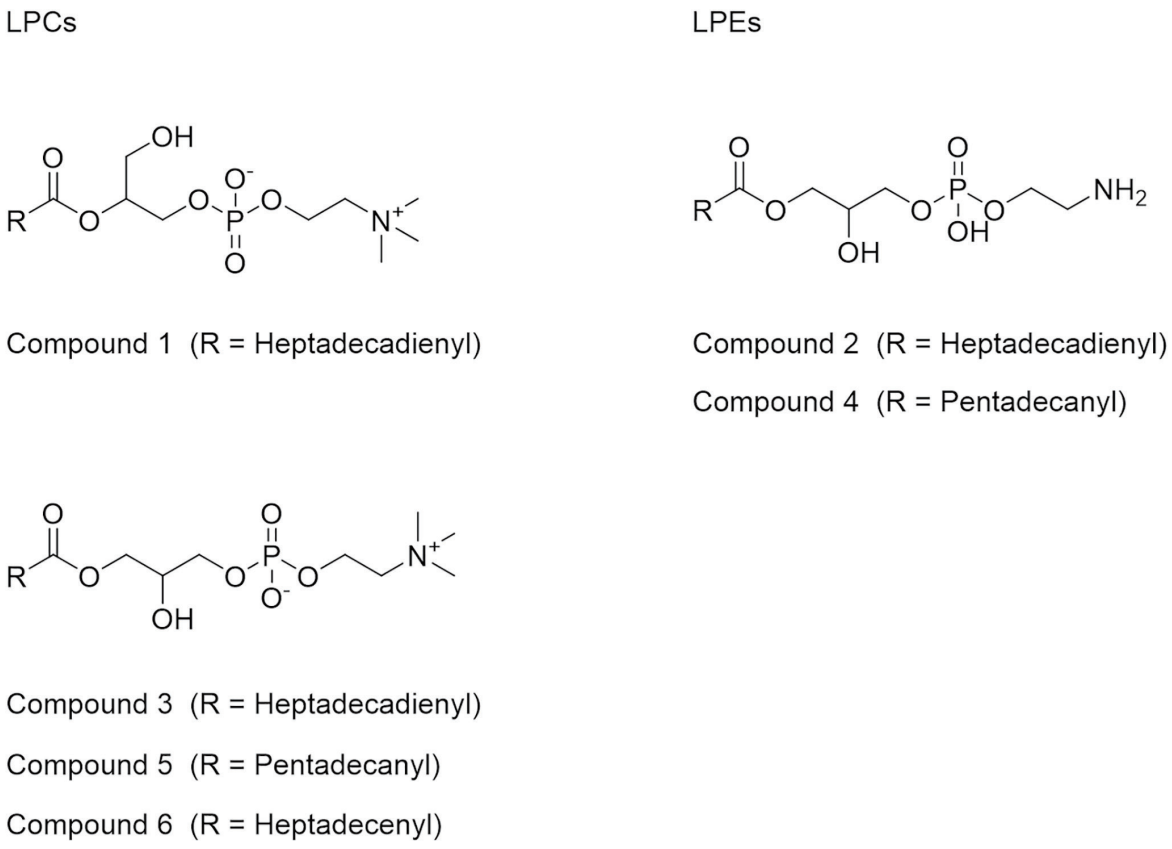

Figure 2. Structures of Key Chemical Constituents in PT Before and After Processing

1) LPC Annotation

Most LPCs exhibit characteristic fragment ions at *m/z* 86, 125, and 184 in the positive ion mode (Suárez-García et al. 2017). These ions were detected in the MS/MS spectra of compounds 1, 3, 5, and 6, confirming their classification as LPCs. Based on their precursor ions (*m/z* 520.3360, 520.3438, 496.3418, and 522.3630, respectively) coupled with the MS/MS characteristic fragment ions, these compounds were annotated as LPC (0:0/18:2) (compound 1), LPC (18:2/0:0) (compound 3),

LPC (16:0/0:0) (compound 5), and LPC (18:1/0:0) (compound 6), respectively (Lin et al. 2021; Xu et al. 2009; Zhai et al. 2019).

Compounds 1 and 3 were selected to investigate the fragmentation behavior of LPCs. In the positive ion mode, compounds 1 and 3 exhibited $[M + H]^+$ ions at *m/z* 520.3360 and 520.3438, respectively. The MS/MS spectrum of compound 1 featured major fragment ions at *m/z* 184.0750, 125.0006, and 86.0971. Compound 3 produced major fragment ions at *m/z* 86.0972, 104.1077, 125.0006, and 184.0743. Based on the observed fragmentation patterns and precursor ion masses, these two compounds were preliminarily annotated as LPC regioisomers (18:2). Between these two compounds, the most abundant fragment ion observed was *m/z* 184 ($[M + H - 336]^+$), corresponding to the phosphocholine ion. The fragment ions at *m/z* 86 ($[M + H - 336 - 98]^+$) and 125 ($[M + H - 336 - 59]^+$) corresponded to the dehydrocholine ion (neutral loss of a phosphate group from phosphocholine ion) and five-membered cyclophosphane ion (neutral loss of trimethylamine from phosphocholine ion), respectively. In addition, a fragment ion at *m/z* 337 ($[M + H - 183]^+$), indicating loss of the phosphocholine group, was detected, supporting the inference that the fatty acid in precursor ion *m/z* 520 is octadecadienoic acid. Compounds 1 and 3 were further distinguished according to the relative intensity of the fragment ion at *m/z* 104, corresponding to the choline ion. The LPC regioisomers *sn*-1 and *sn*-2 (*i.e.*, 1-linoleoyl-*sn*-glycero-3-phosphorylcholine and 2-linoleoyl-*sn*-glycero-3-phosphocholine, respectively) exhibited different cleavage pathways attributable to differences in the acyl chain substitution positions. Specifically, the release of the choline ion (*m/z* 104) in the *sn*-1 regioisomer corresponded to the favored formation of a five-membered cyclic phosphodiester, whereas it was linked to the formation of a six-membered cyclic phosphodiester in the *sn*-2 regioisomer. Because the formation of a five-membered ring is kinetically more favorable, the intensity of the *m/z* 104 ion was significantly greater for the *sn*-1 isomer (Han and Gross 1996). In addition, the peak intensity ratio between *m/z* 104 and 125 significantly differed between the two regioisomers, with ratios of approximately 4:1 for the *sn*-1 isomer and 1:8 for the *sn*-2 isomer (Han and Gross 1996). Based on the fragmentation pattern and related literature, compounds 1 and 3 were annotated as LPC (0:0/18:2) and LPC (18:2/0:0), respectively (Banskota et al. 2022; Han and Gross 1996; Lin et al. 2021; Xu et al. 2009; Zhai et al. 2019). Figures 3 and 4 present the MS/MS spectra and possible fragmentation pathways of LPC (0:0/18:2) (compound 1) and LPC (18:2/0:0) (compound 3).

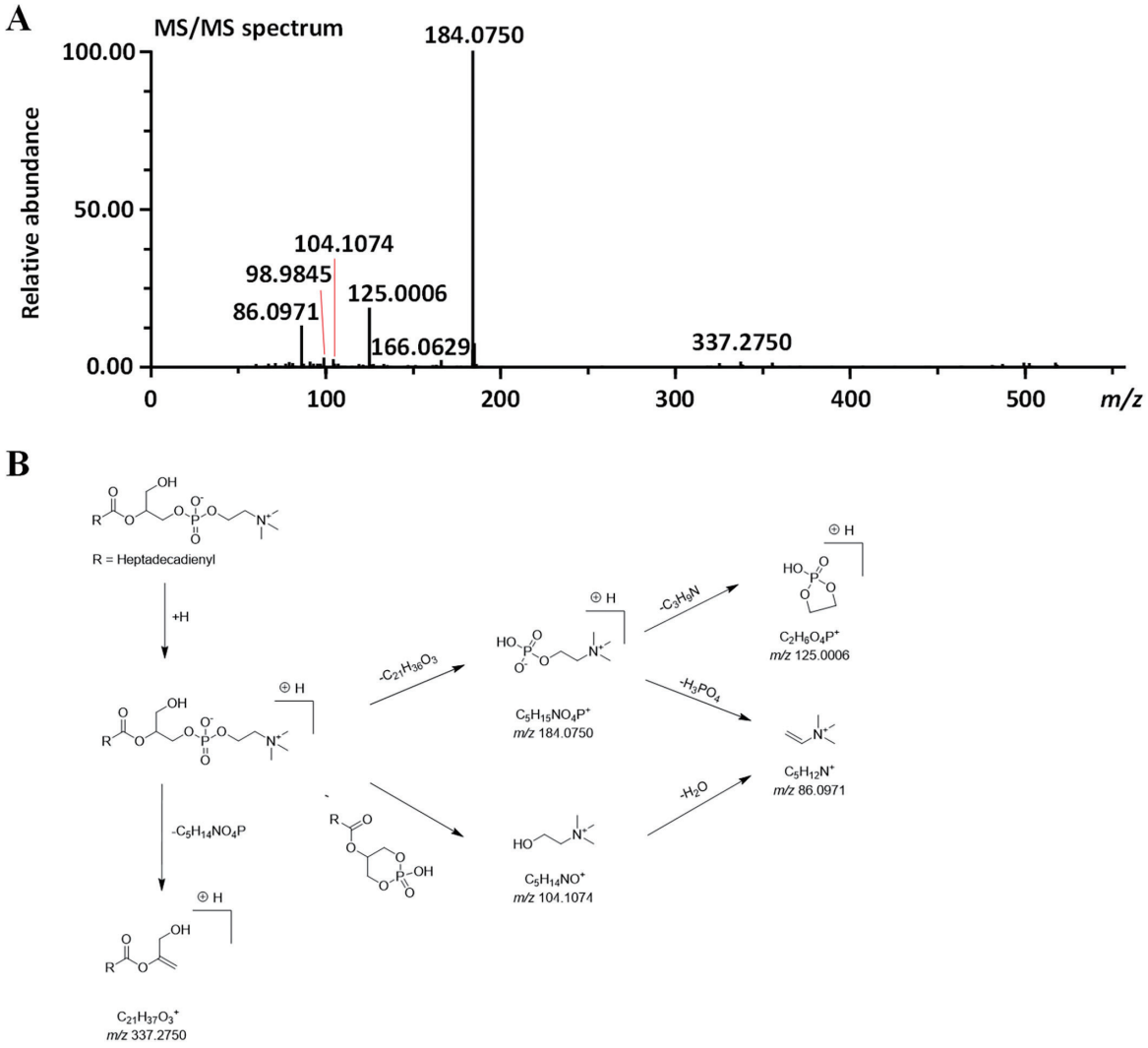

Figure 3. MS/MS Spectrum and Possible Fragmentation Pathways of LPC (0:0/18:2) (Compound 1).

(A) MS/MS spectrum. (B) Possible fragmentation pathways.

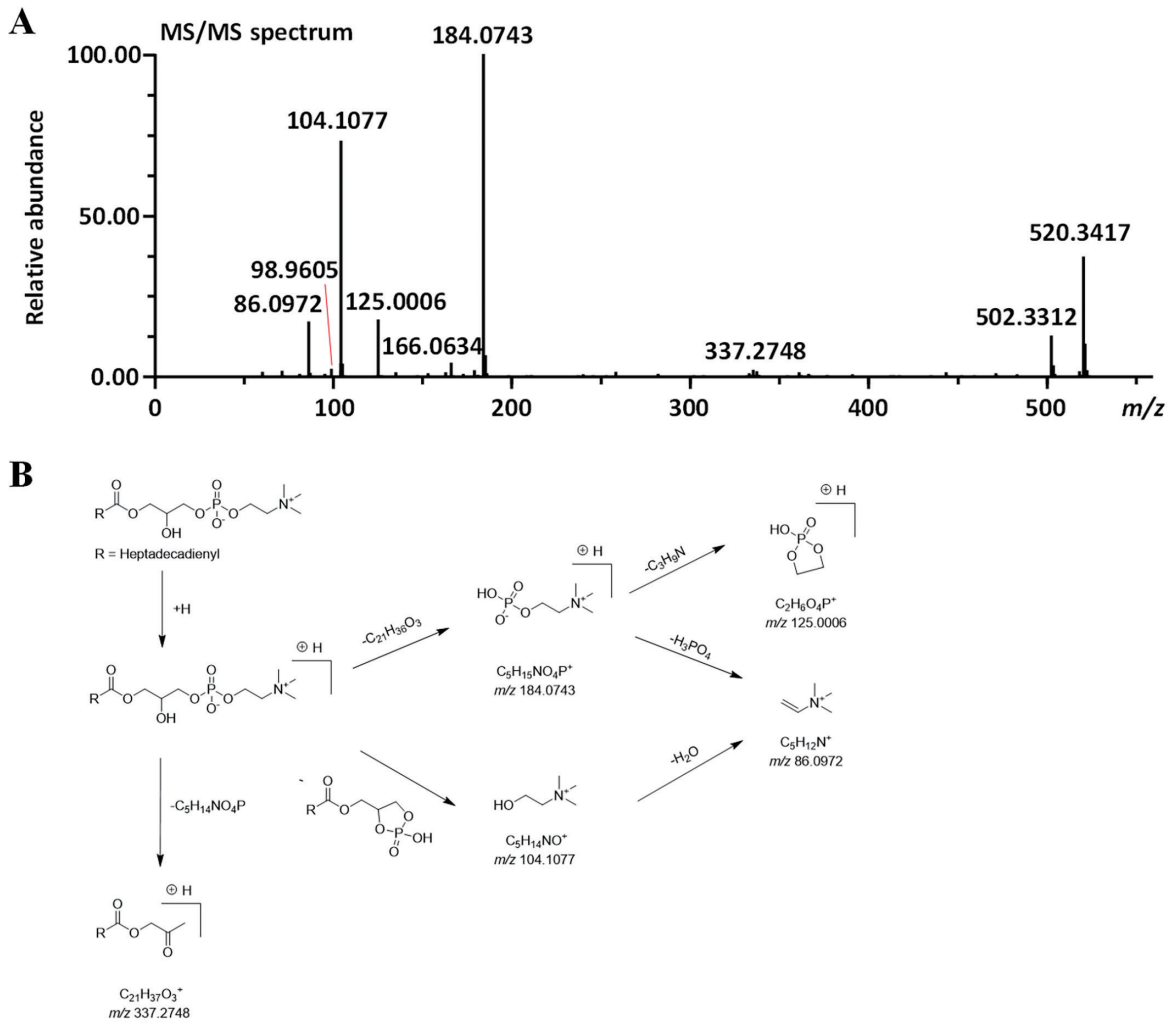

Figure 4. MS/MS Spectrum and Possible Fragmentation Pathways of LPC (18:2/0:0) (Compound 3).

(A) MS/MS spectrum. (B) Possible fragmentation pathways.

2) LPE Annotation

Most LPEs undergo neutral loss of the phosphoethanolamine group (141 Da), thereby generating diagnostic fragment ions in the positive ion mode (Chen et al. 2020; Suárez-García et al. 2017). We selected compound 4 to investigate LPE fragmentation behavior. In the positive ion mode, compound 4 exhibited a $[M + H]^+$ ion at *m/z* 454.2961. The most abundant fragment ion observed at *m/z* 313.2729 ($[M + H - 141]^+$) corresponded to the neutral loss of the phosphoethanolamine group from the precursor ion. In addition, a fragment ion was detected at *m/z* 393.2513 ($[M + H - 61]^+$), corresponding to a neutral loss of 2-aminoethanol from the precursor ion. Based on the fragmentation pattern and related literature, compound 4 was annotated as 3-{[(2-aminoethoxy)(hydroxy)phosphoryl]oxy}-2-hydroxypropyl hexadecanoate (Banskota et al. 2022; Lin et al. 2021; Xie et al. 2012; Yang et al. 2023; Zhai et al. 2019). Figure 5 presents the MS/MS spectrum and possible fragmentation pathways of this compound.

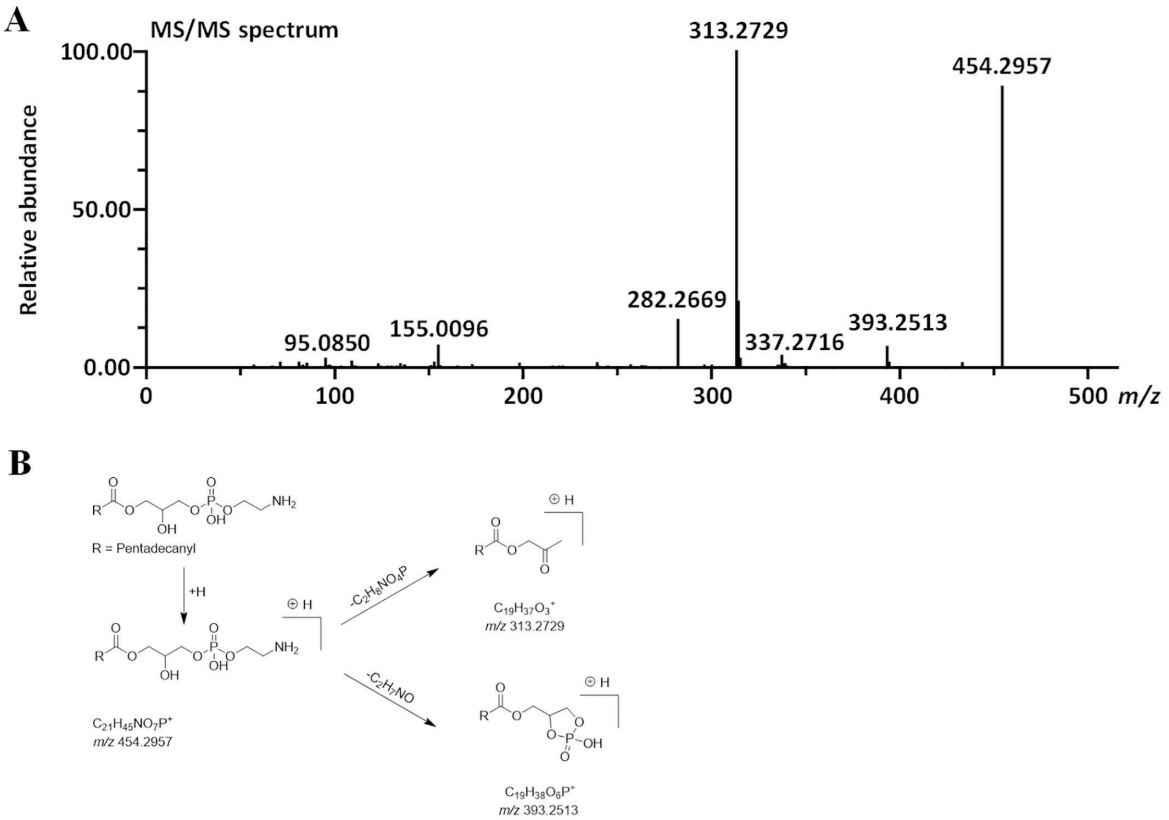

Figure 5. MS/MS Spectrum and Possible Fragmentation Pathways of 3-{[(2-Aminoethoxy) (hydroxy)phosphoryl] oxy}-2-hydroxypropyl Hexadecanoate (Compound 4).
(A) MS/MS spectrum. (B) Possible fragmentation pathways.

3) Fatty Acid Annotation

In the negative ion mode, compounds 7, 8, and 9 exhibited $[M - H]^-$ ions at *m/z* 295.2300, 295.2284, and 295.2276, respectively (all calcd. for $C_{18}H_{31}O_3^-$, 295.2279). The fragment ion at *m/z* 277 ($[M - H - 18]^-$) was detected in all three compounds, corresponding to the neutral loss of H_2O from the precursor ion (Yuan et al. 2013). Additionally, characteristic fragment ions at *m/z* 171, 183, and 195, indicative of hydroxyoctadecadienoic acid, were observed in these three compounds (Yoshida et al. 2008). Based on their fragmentation characteristics and precursor ions, compounds 7, 8, and 9 were annotated as isomers of hydroxyoctadecadienoic acid.

(4) Processing-induced Phospholipid Changes in PT and Their Clinical Relevance

PT processing methods have evolved over time. *Ben Cao Jing Ji Zhu* (本草經集注), compiled during the Qi Dynasty (500 AD), documents simple hot water washing as a PT processing method (Chinese Text Project n.d.b). In addition, the classical text *Qian Jin Yi Fang* (千金翼方, 660 AD) describes this PT processing method, emphasizing the need to remove its slimy mucus to prevent throat irritation (Chinese Text Project n.d.f). Hot water washing likely reduces the irritancy of PT by removing surface mucilage, reducing calcium oxalate crystals, and decreasing P. ternata lectin content (Liu et al. 2023). Meanwhile, *Wan Bing Hui Chun* (萬病回春) lists 142 herbal formulas containing PT, four of which, namely *Jia Jian Dao Tan Tang* (加減導痰湯), *Qian Jin Hua Tan Wan* (千金化痰丸), *Zhu Li Hua Tan Wan* (竹瀝化痰丸), and *Zhu Li Zhi Zhu Wan* (竹瀝枳术丸), specifically use G-APS–treated PT. The majority of the 142 formulas are used for antiemetic purposes, whereas

the four aforementioned formulas are specifically formulated as expectorants. As the bidirectional pharmacological effects of LPCs in gastric mucosal protection and inflammation promotion can exert opposing influences on the antiemetic and expectorant applications of PT, our results indicate that hot water washing and G-APS processing have different effects on LPC content. The metabolic profile of hot water-processed samples remained similar to that of unprocessed samples, mainly exerting a quantitative impact. On the contrary, G-APS processing induced both quantitative and qualitative changes, including a decrease in the relative LPC content. Given the role of LPCs as precursors to LPA, a compound that protects against indomethacin-induced gastric cell damage in medicinal herbs such as Peony root, Cimicifuga rhizome, Panax rhizome, and PT (Afroz et al. 2018), this finding has important implications. Whereas LPCs themselves lack direct gastroprotective activity, they are metabolized by ATX in plasma to LPA, which is believed to exert the observed physiological effects (Nakanaga et al. 2010). This suggests a clinical advantage in using PT as an antiemetic when the overall LPC profile remains qualitatively preserved. Nevertheless, LPCs, particularly saturated and monounsaturated acyl species, promote inflammatory responses by inducing the production of inflammatory mediators, thereby contributing to the development and progression of various inflammatory diseases (Liu et al. 2020; Matsumoto et al. 2007). Clinically, phlegm is often linked to airway mucosal inflammation or irritation. Unlike physiological mucus, pathological sputum is a hallmark of chronic inflammatory respiratory diseases, such as asthma, chronic obstructive pulmonary disease, and cystic fibrosis (Rose and Voynow 2006; Voynow and Rubin 2009). Hence, to inhibit phlegm production associated with throat inflammation, PT with quantitatively and qualitatively lower LPC content could offer a greater therapeutic advantage (Tanaka et al. 2013).

G-APS treatment resulted in significant quantitative and qualitative changes in LPC and LPE content, likely through aluminum, a strong Lewis acid, coordinating with negatively charged phosphate groups to form complexes and induce structural changes in both moieties (Luque et al. 2014). Conversely, negligible qualitative changes in LPC content were observed in the hot water washing group, but the extraction yield was reduced. This is believed to reflect the overall loss of water-soluble chemical components attributable to exposure to large amounts of water during processing. Despite its clinical relevance, the historical processing of crude drugs remains poorly understood. This study offers insights into the pharmacological rationale underlying traditional PT processing methods.

4. Conclusion

Our data demonstrated that hot water washing and G-APS processing exert distinct effects on LPC content in PT. Hot water washing was associated with a similar metabolic profile to that in unprocessed samples, mainly exerting a quantitative impact on LPC content. In contrast, G-APS processing led to both quantitative and qualitative changes in LPC levels. Given the bidirectional pharmacological effects of LPCs in gastric protection and inflammation, processing-induced qualitative differences in LPC profiles could explain the different clinical applications of PT. For antiemetic purposes, PT with a qualitatively preserved LPC profile could be beneficial, owing to the *in vivo* conversion of LPC to LPA, which is associated with gastric mucosal protection, thereby likely contributing to PT's antiemetic effects. Conversely, for expectorant purposes, such protective effects are not expected. Given the pro-inflammatory activity of LPCs, quantitative and qualitative reductions in their content following G-APS processing might be beneficial for clinical treatments targeting phlegm resolution. The marked quantitative and qualitative changes in LPC levels following G-APS processing likely result from aluminum's strong Lewis acidity,

which favors coordination with the phosphate groups in these compounds, leading to structural alterations. Overall, our findings indicate that the selection of PT processing methods should align with detoxification efficiency and the intended therapeutic applications. Furthermore, excessive processing aimed at detoxification requires careful consideration, as it can concurrently reduce therapeutic efficacy. In addition, LPC content could represent a quality marker for the standardization and quality control of processed PT products.

References

Afroz, S., A. Yagi, K. Fujikawa, M. M. Rahman, K. Morito, T. Fukuta, S. Watanabe, E. Kiyokage, K. Toida, T. Shimizu, T. Ishida, K. Kogure, A. Tokumura, and T. Tanaka. 2018. Lysophosphatidic Acid in Medicinal Herbs Enhances Prostaglandin E_2 and Protects against Indomethacin-Induced Gastric Cell Damage *in Vivo* and *in Vitro*. *Prostaglandins & Other Lipid Mediators*, 135, 36–44. <https://doi.org/10.1016/j.prostaglandins.2018.01.003>

Ahmad, M. U., S. M. Ali, A. Ahmad, S. Sheikh, and I. Ahmad. 2015. Lysophospholipids: Advances in Synthesis and Biological Significance. *Polar Lipids*, (2015), 349–389. <https://doi.org/10.1016/B978-1-63067-044-3.50015-7>

Bai, J., J. B. Qi, L. Yang, Z. T. Wang, R. Wang, and Y. H. Shi. 2022. A Comprehensive Review on Ethnopharmacological, Phytochemical, Pharmacological and Toxicological Evaluation, and Quality Control of *Pinellia ternata* (Thunb.) Breit. *Journal of Ethnopharmacology*, 298, 115650. <https://doi.org/10.1016/j.jep.2022.115650>

Banskota, A. H., A. Jones, J. P. M. Hui, R. Stefanova, and I. W. Burton. 2022. Analysis of Polar Lipids in Hemp (*Cannabis sativa* L.) By-Products by Ultra-High Performance Liquid Chromatography and High-Resolution Mass Spectrometry. *Molecules*, 27(18), 5856. <https://doi.org/10.3390/molecules27185856>

Chen, X., Y. D. Yin, Z. W. Zhou, T. Z. Li, and Z. J. Zhu. 2020. Development of a Combined Strategy for Accurate Lipid Structural Identification and Quantification in Ion-Mobility Mass Spectrometry Based Untargeted Lipidomics. *Analytica Chimica Acta*, 1136, 115–124. <https://doi.org/10.1016/j.aca.2020.08.048>

Chinese Pharmacopoeia Commission. 2020. *Pharmacopoeia of the People's Republic of China 2020 Edition*. Beijing: China Medical Science and Technology Press. (In Chinese).

Chinese Text Project n.d.a. *Jin Gui Yu Han Jing* (Classic of the Golden Chamber and Jade Case, 金匱玉函經). <https://ctext.org/wiki.pl?if=gb&res=618713> (accessed April 15, 2025). (In Chinese).

Chinese Text Project n.d.b. *Ben Cao Jing Ji Zhu* (Collective Commentaries on Classics of Materia Medica, 本草經集注). <https://ctext.org/wiki.pl?if=gb&res=987826> (accessed April 15, 2025). (In Chinese).

Chinese Text Project n.d.c. *Liu Juan Zi Gui Yi Fang* (Liu Juanzi's Ghost-Bequeathed Prescriptions, 劉涓子鬼遺方). <https://ctext.org/wiki.pl?if=gb&res=160762> (accessed April 15, 2025). (In Chinese).

Chinese Text Project n.d.d. *Ying Tong Bai Wen* (A Hundred Questions about Infants and Children, 嬰童百問). <https://ctext.org/wiki.pl?if=gb&res=695754> (accessed May 12, 2025). (In Chinese).

Chinese Text Project n.d.e. *Wan Bing Hui Chun* (Restoration of Health from the Myriad Diseases, 萬病回春). <https://ctext.org/wiki.pl?if=gb&res=67400> (accessed April 15, 2025). (In Chinese).

Chinese Text Project n.d.f. *Qian Jin Yi Fang* (Supplement to Prescriptions Worth a Thousand Gold Pieces, 千金翼方). <https://ctext.org/wiki.pl?if=gb&res=358699> (accessed April 15, 2025). (In Chinese).

Fueki, T., I. Nose, Y. Liu, K. Tanaka, T. Namiki, and T. Makino. 2022. Oxalic Acid in Ginger Specifically Denatures the Acrid Raphides in the Unprocessed Dried Tuber of *Pinellia ternata*. *Acupuncture and Herbal Medicine*, 2(1), 33–40. <https://doi.org/10.1097/HM9.0000000000000025>

Fueki, T., K. Tanaka, K. Obara, R. Kawahara, T. Namiki, and T. Makino. 2020. The Acrid Raphides in Tuberous Root of *Pinellia ternata* Have Lipophilic Character and are Specifically Denatured by Ginger Extract. *Journal of Natural Medicines*, 74, 722–731. <https://doi.org/10.1007/s11418-020-01425-6>

Han, X., and R. W. Gross. 1996. Structural Determination of Lysophospholipid Regioisomers by Electrospray Ionization Tandem Mass Spectrometry. *Journal of the American Chemical Society*, 118(2), 451–457. <https://doi.org/10.1021/ja952326r>

Lee, J. Y., N. H. Park, W. Lee, E. H. Kim, Y. H. Jin, E. K. Seo, and J. Hong. 2016. Comprehensive Chemical Profiling of *Pinellia* Species Tuber and Processed *Pinellia* Tuber by Gas Chromatography-Mass Spectrometry and Liquid Chromatography-Atmospheric Pressure Chemical Ionization-Tandem Mass Spectrometry. *Journal of Chromatography A*, 1471, 164–177. <https://doi.org/10.1016/j.chroma.2016.10.033>

Li, D. Y., K. X. Cui, H. Meng, X. G. Zhu, and J. P. Yi. 2021. Scientific Analysis of Processing of Pinelliae Rhizoma by Ancient Hot Water Washing Method. *Chinese Journal of Experimental Traditional Medical Formulae*, 27(07), 127–133. <https://doi.org/10.13422/j.cnki.syfjx.20202355> (In Chinese).

Li, X. Y., D. Liang, X. Q. Zhang, X. H. Li, M. Sha, X. M. Zhang, L. P. Guo, W. Y. Gao, and X. Li. 2022. Quality Evaluation of *Pinelliae Rhizoma* Using Network Pharmacology and Multi-Component Quantitative Analysis. *Traditional Medicine Research*, 7(4), 33. <https://doi.org/10.53388/TMR20220416001>

Lin, P., Q. Wang, Y. H. Liu, H. Jiang, W. H. Lv, T. H. Lan, Z. F. Qin, X. S. Yao, and Z. H. Yao. 2021. Qualitative and Quantitative Analysis of the Chemical Profile for Gualou-Xiebai-Banxia Decoction, a Classical Traditional Chinese Medicine Formula for the Treatment of Coronary Heart Disease, by UPLC-Q/TOF-MS Combined with Chemometric Analysis. *Journal of Pharmaceutical and Biomedical Analysis*, 197, 113950. <https://doi.org/10.1016/j.jpba.2021.113950>

Liu, P. P., W. Zhu, C. Chen, B. Yan, L. Zhu, X. Chen, and C. Peng. 2020. The Mechanisms of Lysophosphatidylcholine in the Development of Diseases. *Life Sciences*, 247, 117443. <https://doi.org/10.1016/j.lfs.2020.117443>

Liu, Y., I. Nose, K. Terasaka, T. Fueki, and T. Makino. 2023. Heating or Ginger Extract Reduces the Content of *Pinellia ternata* Lectin in the Raphides of Pinellia Tuber. *Journal of Natural Medicines*, 77, 761–773. <https://doi.org/10.1007/s11418-023-01717-7>

Luque, N. B., J. I. Mujika, E. Rezabal, J. M. Ugalde, and X. Lopez. 2014. Mapping the Affinity of Aluminum (III) for Biophosphates: Interaction Mode and Binding Affinity in 1:1 Complexes. *Physical Chemistry Chemical Physics*, 16(37), 20107–20119. <https://doi.org/10.1039/C4CP02770A>

Matsumoto, T., T. Kobayashi, and K. Kamata. 2007. Role of Lysophosphatidylcholine (LPC) in Atherosclerosis. *Current Medicinal Chemistry*, 14(30), 3209–3220. <https ://doi.org/10.2174/092986707782793899>

Ministry of Health, Labour and Welfare. 2021. *Japanese Pharmacopoeia 18th Edition*. The MHLW Ministerial Notification No. 220.

Nakanaga, K., K. Hama, and J. Aoki. 2010. Autotaxin—An LPA Producing Enzyme with Diverse Functions. *The Journal of Biochemistry*, 148(1), 13–24. <https://doi.org/10.1093/jb/mvq052>

Peng, W., N. Li, E. C. Jiang, C. Zhang, Y. L. Huang, L. Tan, R. Y. Chen, C. J. Wu, and Q. W. Huang. 2022. A Review of Traditional and Current Processing Methods Used to Decrease the Toxicity of the Rhizome of *Pinellia ternata* in Traditional Chinese Medicine. *Journal of Ethnopharmacology*, 299, 115696. <https://doi.org/10.1016/j.jep.2022.115696>

Rose, M. C., and J. A. Voynow. 2006. Respiratory Tract Mucin Genes and Mucin Glycoproteins in Health and Disease. *Physiological Reviews*, 86(1), 245–278. <https://doi.org/10.1152/physrev.00010.2005>

Shi, K. Q., Y. Xiong, X. Qian, Y. F. Zhu, Y. Yao, Q. Zhang, and S. J. Liu. 2024. Analysis of the Material Basis and Efficacy of the Differences in the Preparation of *Pinellia ternata* Before and After Concoction Based on UPLC-Q-TOF-MS/MS and Network Pharmacology. *Journal of Nanjing University of Traditional Chinese Medicine*, 40(02), 153–166. <https://doi.org/10.14148/j.issn.1672-0482.2024.0153> (In Chinese).

Suárez-García, S., L. Arola, A. Pascual-Serrano, A. Arola-Arnal, G. Aragonès, C. Bladé, and M. Suárez. 2017. Development and Validation of a UHPLC-ESI-MS/MS Method for the Simultaneous Quantification of Mammal Lysophosphatidylcholines and Lysophosphatidylethanolamines in Serum. *Journal of Chromatography B*, 1055–1056, 86–97. <https://doi.org/10.1016/j.jchromb.2017.04.028>

Su, T., Y. Tan, M. S. Tsui, H. Yi, X. Q. Fu, T. Li, C. L. Chan, H. Guo, Y. X. Li, P. L. Zhu, A. K. W. Tse, H. Cao, A. P. Lu, and Z. L. Yu. 2016a. Metabolomics Reveals the Mechanisms for the Cardiotoxicity of Pinelliae Rhizoma and the Toxicity-Reducing Effect of Processing. *Scientific Reports*, 6, 34692. <https://doi.org/10.1038/srep34692>

Su, T., W. W. Zhang, Y. M. Zhang, B. C. Y. Cheng, X. Q. Fu, T. Li, H. Guo, Y. X. Li, P. L. Zhu, H. Cao, and Z. L. Yu. 2016b. Standardization of the Manufacturing Procedure for Pinelliae Rhizoma Praeparatum cum Zingibere et Alumine. *Journal of Ethnopharmacology*, 193, 663–669. <https://doi.org/10.1016/j.jep.2016.09.038>

Suzuki, H., J. M. Inadomi, and T. Hibi. 2009. Japanese Herbal Medicine in Functional Gastrointestinal Disorders. *Neurogastroenterology and Motility*, 21(7), 688–696. <https://doi.org/10.1111/j.1365-2982.2009.01290.x>

Tanaka, T., K. Morito, M. Kinoshita, M. Ohmoto, M. Urikura, K. Satouchi, and A. Tokumura. 2013. Orally Administered Phosphatidic Acids and Lysophosphatidic Acids Ameliorate Aspirin-Induced Stomach Mucosal Injury in Mice. *Digestive Diseases and Sciences*, 58, 950–958. <https://doi.org/10.1007/s10620-012-2475-y>

Voynow, J. A., and B. K. Rubin. 2009. Mucins, Mucus, and Sputum. *Chest*, 135(2), 505–512. <https://doi.org/10.1378/chest.08-0412>

Xie, T., Y. Liang, J. A, H. P. Hao, L. S. Liu, X. Zheng, C. Dai, Y. Y. Zhou, T. Y. Guan, Y. N. Liu, L. Xie, and G. J. Wang. 2012. Post Acquisition Data Processing Techniques for Lipid Analysis by Quadrupole Time-Of-Flight Mass Spectrometry. *Journal of Chromatography B*, 905, 43–53. <https://doi.org/10.1016/j.jchromb.2012.08.001>

Xu, F. G., L. Zou, Q. S. Lin, and C. N. Ong. 2009. Use of Liquid Chromatography/Tandem Mass Spectrometry and Online Databases for Identification of Phosphocholines and Lysophosphatidylcholines in Human Red Blood Cells. *Rapid Communications in Mass Spectrometry*, 23(19), 3243–3254. <https://doi.org/10.1002/rcm.4246>

Yang, N., W. Hu, J. He, X. Wu, T. Zou, J. H. Zheng, C. B. Zhao, and M. Wang. 2023. Ultra-High Performance Liquid Chromatography-Quadrupole/Time-of-Flight Mass Spectrometry-Based Lipidomics Reveals Key Lipid Molecules as Potential Therapeutic Targets of *Polygonum cuspidatum* Against Hyperlipidemia in a Hamster Model. *Journal of Separation Science*, 46(9), 2200844. <https://doi.org/10.1002/jssc.202200844>

Yoshida, Y., S. Kodai, S. Takemura, Y. Minamiyama, and E. Niki. 2008. Simultaneous Measurement of F_2-Isoprostane, Hydroxyoctadecadienoic Acid, Hydroxyeicosatetraenoic Acid, and Hydroxycholesterols from Physiological Samples. *Analytical Biochemistry*, 379(1), 105–115. <https://doi.org/10.1016/j.ab.2008.04.028>

Yuan, Z. X., S. I. Rapoport, S. J. Soldin, A. T. Remaley, A. Y. Taha, M. Kellom, J. H. Gu, M. Sampson, and C. E. Ramsden. 2013. Identification and Profiling of Targeted Oxidized Linoleic Acid Metabolites in Rat Plasma by Quadrupole Time-of-Flight Mass Spectrometry. *Biomedical Chromatography*, 27(4), 422–432. <https://doi.org/10.1002/bmc.2809>

Zhai, X. Y., L. Zhang, B. T. Li, Y. L. Feng, G. L. Xu, S. L. Yang, and C. Jin. 2019. Chemical Components in Pinelliae Rhizoma by UPLC-Q-TOF-MS/MS. *Chinese Journal of Experimental Traditional Medical Formulae*, 25(07), 173–183. <https://doi.org/10.13422/j.cnki.syfjx.20190107> (In Chinese).

Zhang, Z. H., Y. Y. Zhao, X. L. Cheng, Z. Dai, C. Zhou, X. Bai, and R. C. Lin. 2013. General Toxicity of Pinellia ternata (Thunb.) Berit. in Rat: A Metabonomic Method for Profiling of Serum Metabolic Changes. *Journal of Ethnopharmacology*, 149(1), 303–310. <https://doi.org/10.1016/j.jep.2013.06.039>